Amino Acids (2011) 41:621–628
DOI 10.1007/s00726-011-0886-2

ORIGINAL ARTICLE

Toward the rational design of molecular rotors ion sensors based on α,γ-cyclic peptide dimers

María Jesús Pérez-Alvite · Manuel Mosquera · Luis Castedo · Juan R. Granja

Received: 11 January 2011 / Accepted: 8 March 2011 / Published online: 31 March 2011

Abstract A dimer-forming self-assembling cyclic hexapeptide with a control register and a large association constant in water is described. The self-assembly process is followed by pyrene-excimer emission and the main diastereomeric dimer present in solution is switched by controlled addition of divalent cations (e.g., Ca, Mg) or oxalic acid.

Keywords Self-assembling · Cyclic peptide · Molecular rotor · γ-Amino acid · Dimer · Excimer

Abbreviations

Acp	3-Aminocyclopentanecarboxylic Acid
CPs	Cyclic peptides
α,γ-D	Dimer of a α,γ-cyclic peptide
DIEA	Diisopropylethylamine
4-DPPBA	4-(Diphenylphosphino)benzoic Acid
ext-TTF	2-[9-(1,3-dithiol-2-ylidene)anthracen-10(*9H*)-ylidene]-1,3-dithiole
Pap	5-(pyren-1-yl)pentanoic acid
PCBA	[6,6]-phenyl-C61-butyric acid
SPN	Self-assembling Peptide Nanotubes
TBAF	Tetrabutylamonium chloride
TBTU	*O*-Benzotriazol-1-yl-*N,N,N′,N′*-tetramethyluronium tetrafluoroborate

Electronic supplementary material The online version of this article (doi:10.1007/s00726-011-0886-2) contains supplementary material, which is available to authorized users.

M. J. Pérez-Alvite · L. Castedo · J. R. Granja (✉)
Departamento de Química Orgánica, Unidad Asociada al CSIC y Centro Singular de Investigación en Química Biológica y Materiales Moleculares, Universidad de Santiago de Compostela, Campus Vida, 15782 Santiago, Spain
e-mail: juanr.granja@usc.es

M. Mosquera
Departamento de Química Física y Centro Singular de Investigación en Química Biológica y Materiales Moleculares, Universidad de Santiago de Compostela, Campus Vida, 15782 Santiago, Spain

Introduction

One of the most fundamental and pressing problems for the implementation of supramolecular synthetic methods in nanotechnological applications concerns the control of self-assembly processes through the design of molecular components and their practical application at the macromolecular level of the supramolecular entities (Zhang 2003). In addition, the use of tools such as fluorescence (Roy et al. 2008) or single molecule detection (Neuman and Nagy 2008) to follow the formation of supramolecular entities and assess their functions is also demanded. In this context, peptides are very important supramolecular building blocks because of their straightforward synthesis and the potential to introduce chemical diversity, as well as the large variety and easy modulation of their 3D structures (Matsui and Gao 2005; Ashkenasy et al. 2006; König and Kilbinger 2007; Ulijn and Smith 2008 and Pazos et al. 2009). β-sheet-forming peptides are particularly interesting, not only because of their relevance to pathological disorders, such as HIV, cancer and neurodegenerative diseases (Stefani and Dobson 2003; Knowles et al. 2007; Hamley 2007; Kolstoe et al. 2009), but also because of their potential use in the manufacture of nanotapes (Smeenk et al. 2005; Whitehouse et al. 2005) or nanotubes (Brea et al. 2010; Bong et al. 2001). The properties of β-sheet structures not only depend on their amino acid

composition but also on their inter-chain relative orientation (Khakshoor and Nowick 2008; Remaut and Waksman 2006 and Searle and Ciani 2004). Control of β-sheet formation and register structure is highly desirable.

In the last few years, we have been working on the design and synthesis of self-assembling peptide nanotubes (SPN) using cyclic peptides (CPs) that contain cyclic γ-amino acids in which the interactions that link the CPs together are β-sheet-type interactions (Amorín et al. 2003, 2005, 2008; Brea et al. 2007a, 2005). In this context, we have found that the β-sheet register plays an important role in electron and energy transfer processes (α,γ-CPs) (Brea et al. 2007b, c, 2011). For example, we estimated the association constant by dimer-induced excimer formation of α,γ-CPs modified with a pyrene on one of the side chains (**α,γ-CP2**). Only one of the three-topoisomeric dimers (**α,γ-D2$_Z$**) allows the pyrene to stack in the appropriate way to form the excimer while the other two emit as single monomers (Scheme 1). Thus, the association constant could only be estimated by considering that the three nonequivalent dimers that were formed in an equimolecular ratio (Brea et al. 2007c). An even more important limitation concerns the electron transfer process between **α,γ-CP3** and **α,γ-CP4**, in which the highly efficient interspace electron transfer only takes place in dimer **α,γ-D3-4$_Z$**, where the fullerene acceptor (PCBA) and the donor (ext-TTF) are oriented in the same direction, while the other two dimers are not active because of the long distance between the two electroactive components (Brea et al. 2007b). So β-sheet register control is highly demanded to fully understand and control self-assembling CP structures. We describe here a new α,γ-CP system with a large association constant, both in organic and aqueous media, and in which the isomeric dimer formed is under control and can be switched on demand.

Materials and methods

(*L*)-2-(*tert*-butoxycarbonylamino)-5-(pyren-1-yl)pent-4-ynoic acid A solution of 4-DPPBA (145 mg, 0.47 mmol), Cs_2CO_3 (1.93 g, 5.93 mmol) in a H_2O/DMF mixture (5:1, 120 mL) was degassed for 15 min under argon and then CuI (321 mg, 1.68 mmol), 10% Pd/C (126 mg, 0.12 mmol) and bromopyrene (1 g, 3.6 mmol) were added and the sample was degassed for another 30 min. (*L*)-2-(*tert*-butoxycarbonylamino)pent-4-ynoic acid (506 mg, 2.37 mmol) was added and the mixture heated at 80°C under argon for 4 h. After cooling at room temperature, the reaction mixture was filtered through a Celite pad, washed with H_2O/DMF mixture. The resulting solution was washed with CH_2Cl_2 and the aqueous phase was lyophilized. The resulting powder was purified by flash chromatography (2% EtOH/CH_2Cl_2 with 0.5% AcOH) to give 783 mg of the (*L*)-2-(*tert*-butoxycarbonylamino)-5-(pyren-1-yl)pent-4-ynoic acid as a yellow foam [80%, Rf = 0.15 (5% MeOH in CH_2Cl_2)]. **^{1}H NMR** (*CD_3OD*, 500.14 MHz, δ): 8.54 (d, J = 9.1 Hz, 1H), 8.22 (t, J = 7.3 Hz, 3H), 8.15 (d, J = 9.1 Hz, 1H), 8.13–8.00 (m, 4H), 4.54 (t, J = 6.0 Hz, 1H), 3.25–3.10 (dq, J = 17.0 and 5.2 Hz, 2H), 1.46 (s, 9H); **^{13}C NMR** (*CD_3OD*, 125.76 MHz,

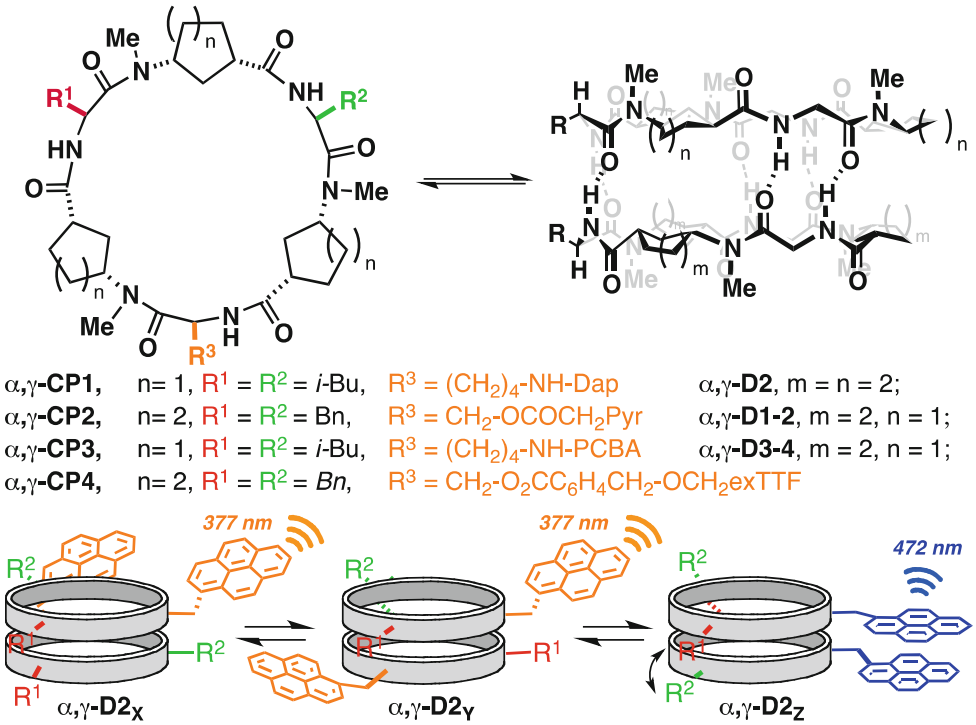

Scheme 1 α,γ-Cyclic peptide (**α,γ-CP**) and dimer (**α,γ-D**) structures used in previous studies (*top*) and model of the equilibrium of the three dimers of **α,γ-CP2** (**α,γ-D2$_x$**, **α,γ-D2$_y$**, **α,γ-D2$_z$**) in which only the former is able to form the pyrene excimer (*bottom*)

δ): 174.3 (CO), 157.8 (CO), 133.1 (C), 132.6 (C), 132.4 (C), 130.8 (CH), 129.3 (CH), 129.0 (CH), 128.2 (CH), 127.4 (CH), 126.6 (CH), 125.5 (CH), 125.4 (CH), 119.3 (C), 92.0 (C), 82.6 (C), 80.8 (C), 62.7 (CH_2), 54.2 (CH), 28.7 (CH_3), 24.2 (CH_2); **FTIR** (293K, $CHCl_3$): 3433, 2983, 2929, 2854, 1722, 1515 cm^{-1}; **MS (ES$^+$)** [m/z (%)]: 436 ($[M + Na]^+$, 36), 414 ($[MH]^+$, 16), 314 ($[MH\text{-}Boc]^+$, 100); **HRMS** $[MH]^+$ **calculated** for $C_{26}H_{24}NO_4$ 414.1700, **found** 414.1703.

(*L*)-2-(*tert*-butoxycarbonylamino)-5-(pyren-1-yl)pentanoic acid (*L*-Boc-Pap-OH) A solution of (*L*)-2-(*tert*-butoxycarbonylamino)-5-(pyren-1-yl)pent-4-ynoic acid (110 mg, 0.27 mmol) in ethanol (9 mL) and acetic acid (45 μL) was degassed for 15 min and then treated with Pd/C (10%, 56 mg) and stirred overnight at room temperature under balloon pressure of hydrogen. The resulting mixture was filtered through a Celite pad, the residue was washed with ethanol, and the filtrates were concentrated under reduced pressure. The reaction crude was purified by flash chromatography (2%EtOH/CH_2Cl_2 with 0.5% AcOH) affording 98 mg of ***L*-Boc-Pap-OH** as a yellow foam [88%, Rf = 0.25 (5% MeOH in CH_2Cl_2)]. **^{1}H NMR** (*CD_3OD,* 500.14 MHz, δ): 8.24 (d, $J = 9.2$ Hz, 1H), 8.10 (d, $J = 7.6$ Hz, 2H), 8.07–8.02 (m, 2H), 7.99–7.90 (m, 3H), 7.82 (d, $J = 7.6$ Hz, 1H), 4.27–4.07 (m, 1H), 3.43–3.15 (m, 2H), 2.08−1.66 (m, 4H), 1.39 (s, 9H); **^{13}C NMR** (*CD_3OD,* 125.76 MHz, δ): 158.2 (CO), 137.6 (CO), 132.8 (CO), 132.4 (CH), 132.3 (CH), 131.2 (CO), 129.8 (CH), 128.5 (CH), 128.4 (CH), 128.3 (CH), 127.6 (CH), 126.9 (CH), 126.2 (C), 126.1 (C), 125.9 (CH), 125.7 (CH), 124.4 (CH), 80.5 (C), 69.1 (CH_2), 40.1 (C), 33.8 (CH_2), 32.8 (CH_2), 31.6 (CH_2), 30.1 (CH_2), 29.3 (CH_2), 28.7 (CH), 24.9 (CH_2), 24.0 (CH_2); **FTIR** (293 K, $CHCl_3$): 3422, 2975, 2928, 2863, 2367, 1722, 1515 cm^{-1}; **MS (ES$^+$)** [m/z (%)]: 440 ($[M + Na]^+$, 100), 418 ($[MH]^+$, 11), 318 ($[MH–Boc]^+$, 58); **HRMS** $[MH]^+$ **calculated for** $C_{26}H_{28}NO_4$ 418.2013 **found** 418.2013.

Peptide synthesis

Linear peptides Boc-[*L*-Pap-*D*-^{Me}*N*-γ-Acp-*L*-Glu(OBn)-*D*-^{Me}*N*-γ-Acp-*L*-Lys(Z)-*D*-^{Me}*N*-γ-Acp-]OFm was prepared following the synthetic strategy previously described (see also Supplementary materials, Amorín et al. 2005 and Brea et al. 2005).

***c*-[*L*-Pap-*D*-^{Me}*N*-γ-Acp-*L*-Glu(OBn)-*D*-^{Me}*N*-γ-Acp-*L*-Lys(Z)-*D*-^{Me}*N*-γ-Acp-] (α,γ-CP5)** A solution of Boc-[*L*-Pap-*D*-^{Me}*N*-γ-Acp-*L*-Glu(OBn)-*D*-^{Me}*N*-γ-Acp-*L*-Lys(Z)-*D*-^{Me}N-γ-Acp-]-OFm (988 mg, 0.68 mmol) in a piperidine/CH_2Cl_2 solution (1:4, 6.9 mL) was stirred at room temperature for 20 min. After removal of the solvent, the residue was dissolved in CH_2Cl_2 (20 mL) and the solution washed with HCl (5%), dried over Na_2SO_4, filtered and concentrated. The resulting residue was dissolved in a TFA/CH_2Cl_2 mixture (1:1, 6.9 mL) and stirred at room temperature for 15 min. After removal of the solvents, the residue was dried under high vacuum and used without further purification. The linear peptide was dissolved in CH_2Cl_2 (688 mL) and treated with HATU (288 mg, 0.76 mmol), followed by dropwise addition of DIEA (720 μL, 4.19 mmol). The resulting mixture was stirred for 10 h at room temperature to complete the reaction and then the solvent was removed under reduced pressure. The resulting residue was purified by HPLC, affording 500 mg of **α,γ-CP5** as a white solid [63%, $R_t = 13$ min (Phenomenex Maxsil-10 silica semipreparative column, 7–12% MeOH in CH_2Cl_2, 25 min)]. **^{1}H NMR** (*$CDCl_3$,* 500.14 MHz, δ): 8.40–7.68 (m, 12H, 3NH, Pyr), 7.37−7.27 (m, 8H, Bn), 7.25–7.20 (m, 2H, Bn), 5.32−4.92 (m, 7H, CH_2-Bn, α-Prg, Glu and Lys), 4.86–4.67 (m, 3H, H_γ Acp), 3.42–3.22 (m, 2H, CH_2-Pyr), 3.17–3.08 (m, 2H, CH_2-Lys), 3.05–2.96 (m, 9H, CH_3), 2.96–2.87 (m, 3H, H_α Acp), 2.46–2.21 (m, 6H, Acp), 2.22–1.98 (m, 4H), 1.97–1.11 (m, 30H); **^{13}C NMR** (*$CDCl_3$*, 125.76 MHz, δ): 175.4 (CO), 175.3 (CO), 173.1 (CO), 172.5 (CO), 156.5 (CO), 136.5 (C), 136.2 (C), 135.9 (C), 135.6 (C), 131.3 (CH), 130.8 (CH), 129.7 (CH), 128.5 (CH), 128.4 (CH), 128.2 (CH), 128.0 (CH), 128.0 (CH), 127.4 (CH), 127.2 (CH), 126.6 (CH), 125.8 (CH), 124.7 (CH), 123.3 (CH), 123.1 (CH), 66.5 (CH_2), 54.8 (CH), 50.2 (CH), 48.3 (CH), 47.8 (CH), 42.5 (CH_2), 42.3 (CH), 40.6 (CH_2), 35.9 (CH_2), 33.0 (CH_2), 30.2 (CH_3), 29.9 (CH_3), 29.8 (CH_3), 28.3 (CH_2), 27.6 (CH_2), 27.1 (CH_2), 26.9 (CH_2), 22.5 (CH_2); **FTIR** (293K, $CHCl_3$): 3435, 3302, 2943, 2873, 2359, 1718, 1620, 1525 cm^{-1}; **MS (ES$^+$)** [m/z (%)]: 1156 ($[MH]^+$, 100), 578 ($[MH]^{2+}$, 23); **HRMS** $[MH]^+$ **calculated for** $C_{68}H_{82}N_7O_{10}$ 1156.6118, **found** 1156.6111.

***c*-[*L*-Pap-*D*-^{Me}*N*-γ-Acp-*L*-Glu-*D*-^{Me}*N*-γ-Acp-*L*-Lys-*D*-^{Me}*N*-γ-Acp-] (α,γ-CP6)** To a mixture of *c*-[*L*-Pap-*D*-^{Me}*N*-γ-Acp-*L*-Glu(OBn)-*D*-^{Me}*N*-γ-Acp-*L*-Lys(Z)-*D*-^{Me}*N*-γ-Acp-] (**α,γ-CP5**) (429 mg, 0.37 mmol), pentamethylbenzene (429 mg, 2.89 mmol) and anisole (430 μL, 4 mmol) in TFA (43 mL) was treated with HBr/AcOH (33%, 8.6 mL, 45 mmol). After stirring 4 h at room temperature, the solvent was removed under reduced pressure, and the crude was purified by HPLC, affording 215 mg of **α,γ-CP6** as a white solid [50%, $R_t = 29$ min (Sugelabor Inertsil C18 column, 60–85% MeOH in H_2O)]. **^{1}H NMR** (*DMSO: $CDCl_3$* (20:80), 500.14 MHz, δ): 8.31–7.63 (m, 12H), 4.93-4.65 (m, 3H), 2.96–2.82 (m, 4H), 2.78–2.61 (m, 3H), 2.55–2.46 (m, 6H), 2.22–2.12 (m, 1H), 1.99–0.97 (m, 18H); **^{13}C NMR** (*DMSO: $CDCl_3$ (30:70)*, 125.76 MHz, δ): 173.1 (CO), 172.4 (CO), 170.3 (CO), 170.0 (CO), 134.8 (C), 129.3 (C), 128.8 (C), 127.7 (C), 126.5 (CH), 125.7 (CH), 125.4 (CH), 124.8 (CH), 124.2 (CH), 123.1 (CH),

122.9 (CH), 122.8 (CH), 121.7 (CH), 52.3 (CH), 46.7 (CH), 46.4 (CH), 40.3 (CH_2), 32.3 (CH_2), 31.0 (CH_3), 30.3 (CH_2), 29.8 (CH_2), 28.2 (CH_2), 27.4 (CH_2), 26.0 (CH_2), 25.6 (CH_2), 25.3 (CH_2), 25.2 (CH_2), 20.6 (CH_2); **FTIR** (293K, $CHCl_3$): 3429, 3294, 2956, 2866, 1684, 1620, 1543 cm^{-1}; **MS (ES$^+$)** [m/z (%)]: 972 ($[M + K]^+$, 7), 955 ($[M + Na]^+$, 100), 933 ($[MH]^+$, 34); **HRMS** $[MH]^+$ **calculated** for $C_{53}H_{70}N_7O_8$ 932.5280, **found** 932.5265.

Time-resolved fluorescence

Fluorescence lifetimes were determined by time-correlated single-photon counting on an Edinburgh Instruments CD-900 spectrometer equipped with a hydrogen-filled nanosecond flash lamp. The instrumental response width of the system is 1.0 ns. We measured usually until 10,000 counts were reached in (2 × 103 channels). The emission band-pass for the lifetime measurements was usually 20 nm. The experiments were performed at room temperature, and samples were purged with argon prior to measurement.

Results and discussion

In order to control the dimeric species formed in solution, we considered that the inter-strand side-chain/side-chain interactions are very different in the three possible dimers (**α,γ-D2$_X$**, **α,γ-D2$_Y$** and **α,γ-D2$_Z$**) (Reiriz et al. 2009 and Garcia-Fandiño et al. 2009). For example, the R^1 side chains (in red) of the excimer-forming dimer (**α,γ-D2$_Z$**) are cross-strand closed to R^2 side chains (in green), and this pairing type is not present in any of the other dimers (Scheme 1). We envisaged that the presence of attractive interactions between the R^1 and R^2 side chains would favor the formation of **α,γ-D$_Z$**, thus inducing the approximation of the remaining side chain. Based on these considerations, we designed a new CP (**α,γ-CP6**) in which R^1 could be a side chain bearing a carboxylic acid group (Glu), meaning that R^2 should be a side chain containing a basic group such us Lys (Scheme 2). To follow the self-assembly process and dimer control, we included in the third amino acid a pyrene group.

The pyrenylamino acid (***L*-Boc-Pap-OH**) used for this study was prepared from Boc-propargylglycine by means of a Sonogashira cross-coupling reaction with 1-bromopyrene and 10% Pd on carbon in an aqueous medium (López-Deber et al. 2001; Brea et al. 2006), followed by hydrogenation (10% Pd on carbon) in 1% acetic acid in ethanol (Scheme 2). The resulting (*L*)-2-(*tert*-butoxycarbonylamino)-5-(pyren-1-yl)pentanoic acid has a higher fluorescence quantum yield than the pyreneacetic esters used in previous studies (Brea et al. 2007c, 2010; Masuko et al. 2000, Nakamura et al. 2008; Kashida et al. 2010 and Valeur 2002). The solution-phase synthesis of a linear peptide, using a strategy similar to that previously reported (see Scheme 1 SI in supporting information) (Amorín et al. 2005 and Brea et al. 2005), and cyclization with TBTU of the resulting linear peptide provided **α,γ-CP5**. Treatment of this peptide with HBr in acetic acid gave unprotected **α,γ-CP6**. Fully protected **α,γ-CP5** has similar self-assembly properties to previously reported CPs, with a K_a value in chloroform of 1.6 × 10^6 M^{-1}, which was determined by

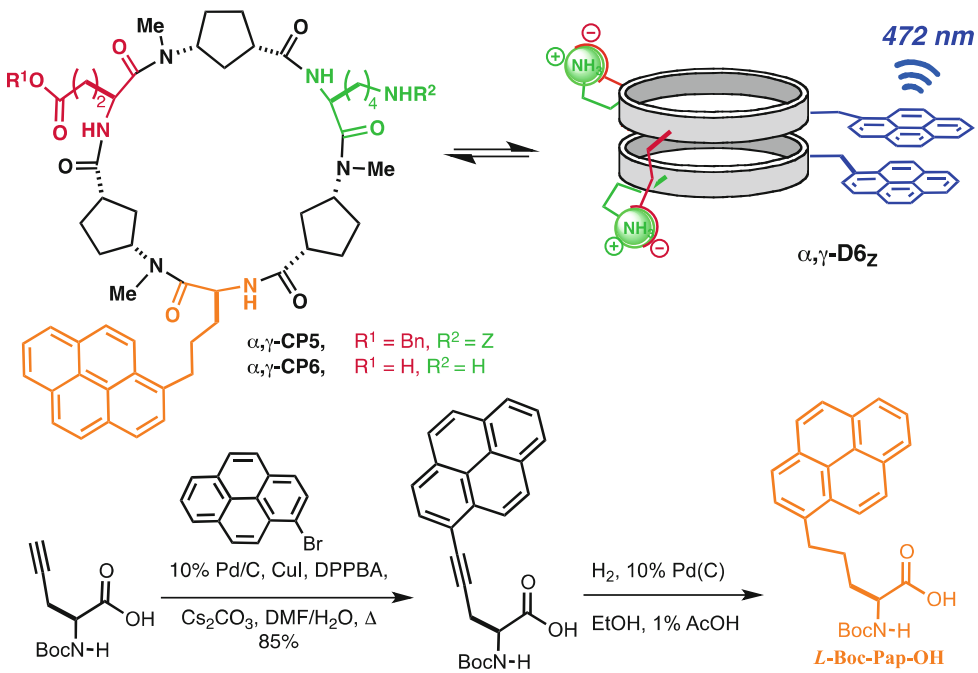

Scheme 2 Structure of **α,γ-CP5** and **α,γ-CP6** and proposed model for the structure of **α,γ-D6$_Z$**; the strategy for the synthesis of N-Boc-5-pyrenyl-2-aminopentanoic acid is shown at the bottom

least-squares analysis fitting to appropriate equations using Kaleidagraph 3.5 (Synergy Software, Reading, PA, USA), (Figure 1 SI in supporting information) (Park et al. 2003 and Martin 1996). The ratio between the three nonequivalent dimers (**α,γ-D5$_x$**, **α,γ-D5$_y$**, **α,γ-D5$_z$**) could not be established by NMR studies but assumed to be equimolar. On the other hand, the low solubility of unprotected peptide **α,γ-CP6** precluded the measurement of its K_a in chloroform. However, this compound has an association constant of $4.5 \times 10^5\ M^{-1}$ in 20% DMSO/$CHCl_3$ (Fig. 1b) and shows, as expected, an increased dimerization constant (association constant in similar conditions (20% DMSO/$CHCl_3$) of **α,γ-CP5** was estimated to be $4.8 \times 10^4\ M^{-1}$, although this was measured at peptide concentrations that are above the region in which rigorous quantitative analysis is possible) that can be attributed to the establishment of the salt bridge interactions. It should be pointed out that the association constant of **α,γ-CP6** is pH dependent, so the 0.12 mM solution (20% DMSO/$CHCl_3$) of the reverse phase purified **α,γ-CP6**, in which amino and carboxylic acid groups are protonated, presents a low excimer signal that increases markedly on addition of small amounts of base (DIEA) (Fig. 1a). The presence of a large excess of DIEA leads to a reduction in the excimer signal.

Additionally, **α,γ-CP6** was soluble in water and excimer emission (Shiraishi et al. 2006) was detected even at a low micromolar concentration, with an association constant at pH 5.4 of $1.4 \times 10^4\ M^{-1}$ (Fig. 1d and Figure 2 SI in supporting information) that it is slightly more acidic than the espected considering the pKa of Lys (10.5) and Glu (4.55) in the dimeric structure (Hui et al. 2005; Delphine et al. 2008). Once again, the self-assembly process is pH-dependent but there is a more pronounced reduction under

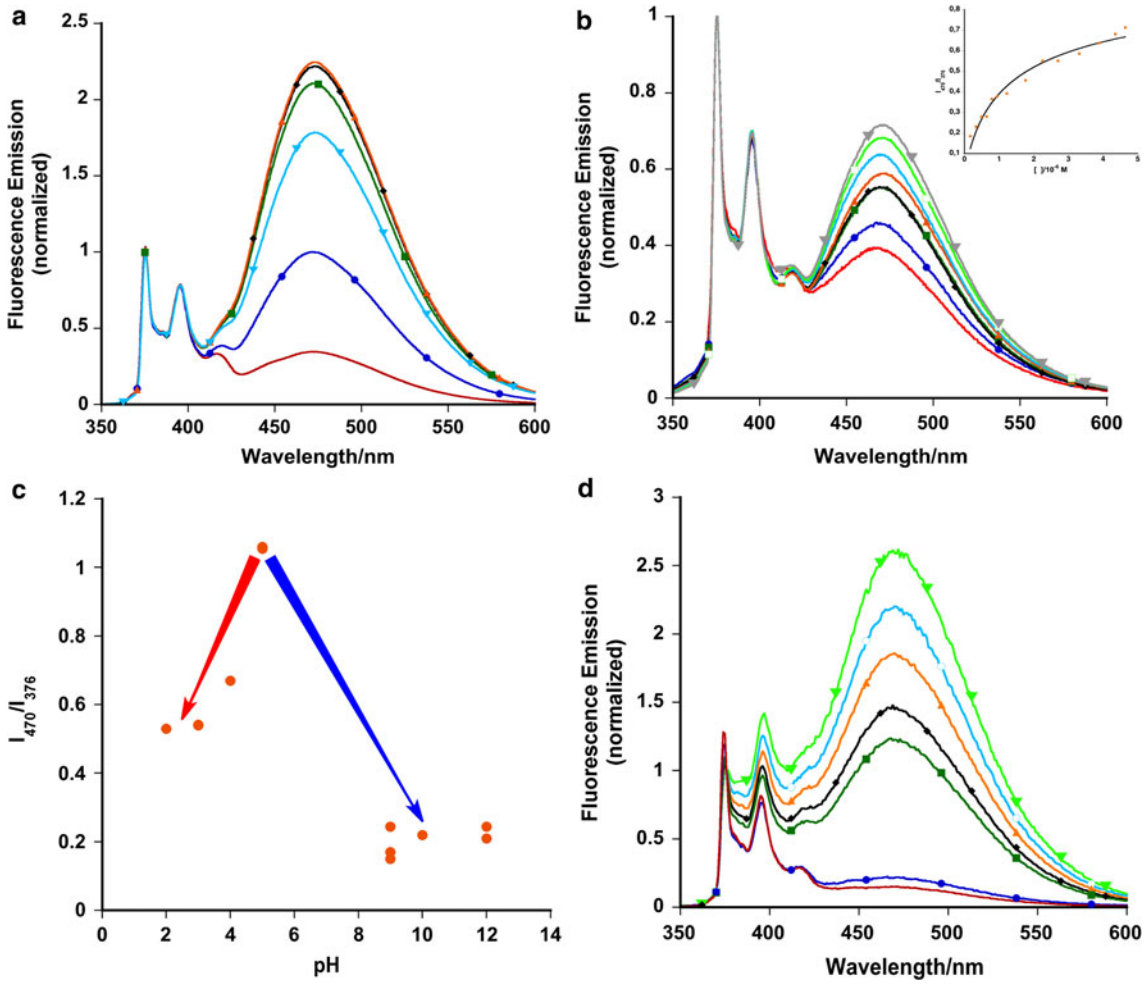

Fig. 1 **a** Pyrene fluorescence emission (337 nm excitation wavelength) of 1.2 μM **α,γ-CP6** in 20% DMSO/$CHCl_3$ (*red lines*) and upon addition of 1.8 (*dark blue circles*), 3.5 (*green squares*), 5.3 (*black diamonds*), 7.1 (*orange lines*) and 28.3 (*light blue lines*) equiv of DIEA. **b** Emission of **α,γ-CP6** in 20% DMSO/$CHCl_3$ (340 nm excitation wavelength), from 1.2 μM (*red lines*) to 45 μM (*grey inverted triangles*), denoting dimer formation. Insert shows titration for K_a calculation. **c** pH dependence of the emission of excimer of **α,γ-D6** (40 μM) in water solution (35 mM NaCl) regulated by the addition of NaOH (1 M) and HCl (1 M) to the neutral solution. **d** Emission of **α,γ-CP6** in 10 mM phosphate buffer, 100 mM NaCl at pH 5.6 (340 nm excitation wavelength), from 7.1 μM (*red lines*) to 83.0 μM (*light green inverted triangles*)

basic conditions than in acidic media, with the optimal conditions identified at pH 5.4 (Fig. 1c).

Time-resolved fluorescence techniques in nonpolar solvents ($CHCl_3$) showed a triexponential fluorescence decay at the excimer emission wavelength (475 nm, see Fig. 2a and Figure 3 SI in supporting information) (Brea et al. 2007c, 2011). The shorter lifetimes (2.0 and 7.6 ns) show negative amplitudes, which must be assigned to the formation of the excimer. The longer lifetime (22.8 ns) shows positive amplitude and must correspond therefore to the excimer decay. We interpret the fact that two different rate constants contribute to the excimer formation process as indicative of the geometrical rearrangements that are needed for excimer formation (Brea et al. 2007c, 2011). This result suggests that in nonpolar media the pyrene side chains are not pre-organized in a stacked structure, which is only formed in the excited state due to the greater interaction between the molecules of pyrene when one of them is in the first excited singlet state (excimer interaction). Based on this, we assume that the π-π stacking interaction of the aromatic moieties is undetectable in organic solvents and is therefore not contributing to stabilization of the dimer structure. A completely different behavior is found in aqueous solution, as deduced from the monoexponential decay of the excimer fluorescence (65.0 ns, Fig. 2a and Figure 4 SI in supporting information). The non-observation of a rise-time in the fluorescence decay emission of the excimer in water implies that the pyrene moieties are already stacked in the electronic ground state, i.e., the hydrophilic solvent favors the stacking interaction of the pyrene moieties. This fact causes the much greater contribution of the excimer band to the fluorescence spectrum in water as compared to organic solvents (the excimer/monomer intensity ratio (I_E/I_M), which was calculated from the fluorescence intensity of the monomer (376 nm) and excimer (470 nm), takes a value of 18 in water and 2.5 in $CHCl_3$). A monoexponential decay was also observed for the pyrene emission wavelength (380 nm) with a long life-time factor (100 ns) compared to organic solutions (Figure 4 SI in supporting information), confirming that there is no interconversion between the monomer emitting form to the excimer one.

Finally, we decided to study the control and switching of the dimer register by altering external signals (Zhang et al. 2009). At neutral pH, **α,γ-CP6** ($2.5\ 10^{-5}$ M) self-assembles into the corresponding excimer-emitting dimer (**α,γ-D6$_Z$**), as discussed above (Scheme 3). Addition of divalent cations, such as Ca^{2+} ($CaCl_2$), Ba^{2+} [$Ba(CF_3SO_3)_2$] or Mg^{2+} ($MgCl_2$), led to the disappearance of the excimer signal (Fig. 2b) and an increase in the monomer band. These changes are attributed to the formation of **α,γ-D6$_X$.Ca^{2+}** as a result of the coordination of the two carboxylic side chains with the divalent cations. Addition of monovalent cations, such as Na^+ or K^+, or even divalent ions such like Zn^{2+}, did not cause any noteworthy change in either the excimer emission or the dimer register. The calcium-coordinated dimer (**α,γ-D6$_X$.Ca^{2+}**) can revert to the *Z*–form (**α,γ-D6$_Z$**) by treatment with tetrabuylammonium fluoride, which induces the precipitation of CaF_2 and restores the excimer emission. On the other hand, the addition of oxalic acid or its sodium salt to the **α,γ-D6$_Z$** solution (1×10^{-5} M) again caused a reduction in the emission of the 470 nm band (Figure 5SI in supporting information). In this case, the double salt bridge interaction between Lys side chains with the carboxylates of oxalate

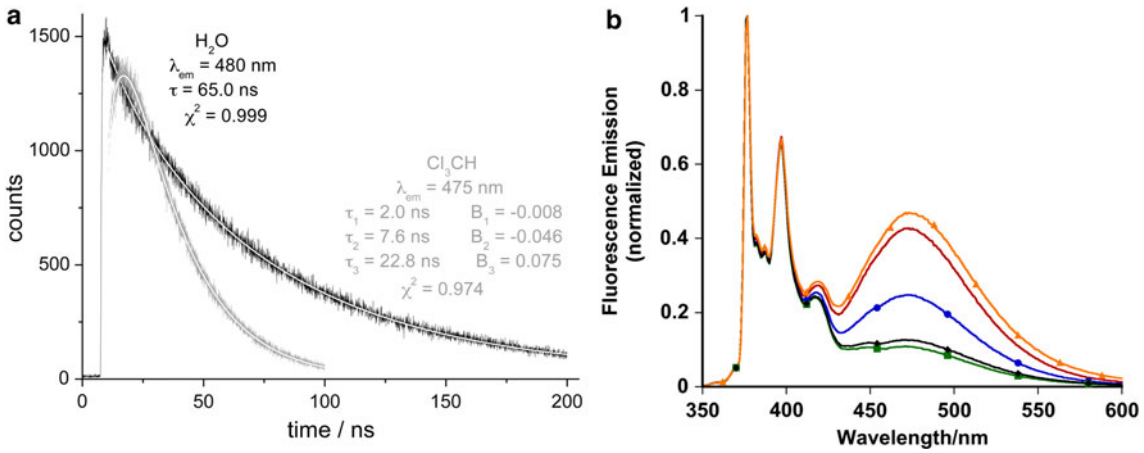

Fig. 2 **a** Fluorescence decay of 5 μM **α,γ-D6** in chloroform (475 nm, *black*) and in water (480 nm, *grey*), with excitation at 333 nm. **b** Pyrene fluorescence emission (337 nm excitation wavelength) of 2.5×10^{-5} M **α,γ-CP6** in 30% DMSO:$CHCl_3$ (*red lines*) upon addition of 1.1 (*blue circles*), 3.4 (*green squares*) equiv of calcium chloride and 1.1 (*black diamonds*) and 10 (*orange inverted triangles*) equivalent of TBAF, suggesting switching between dimer **α,γ-D6$_z$** and **α,γ-D6$_x$** (see Scheme 3)

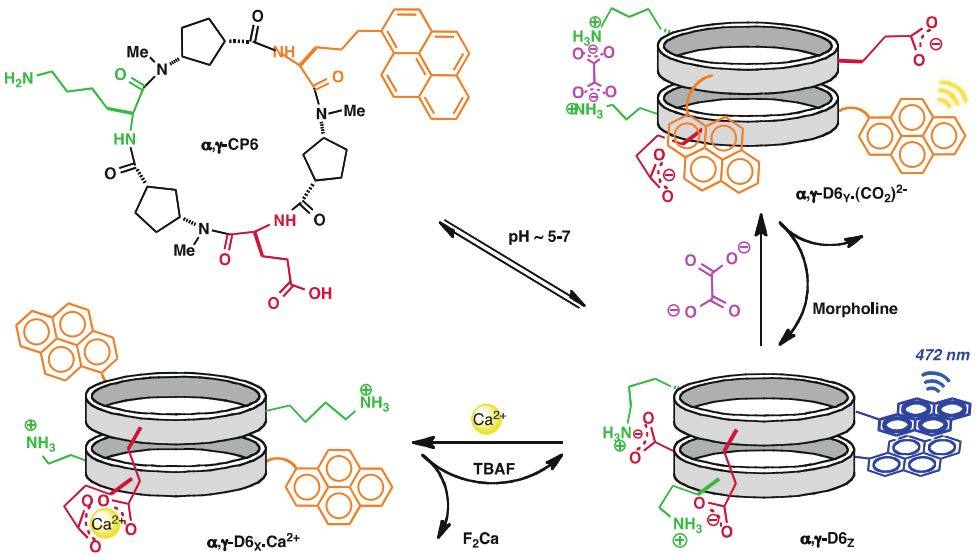

Scheme 3 Representation of inter-dimer interconversion of **α,γ-D6$_x$**, **α,γ-D6$_y$** and **α,γ-D6$_z$** through the addition of different chemical signals (Ca^{2+}/TBAF or oxalate/morpholine)

must be responsible for the swap to the *Y*-form dimer [**α,γ-D6$_y$.(CO$_2$)$^{2-}$**]. Addition of similar amounts of acetic acid or sodium acetate to the **α,γ-D6$_Z$** dimer did not induce any significant change in the excimer emission, suggesting that the previously observed dimer switching is neither due to the ionic strain of the media nor due to pH changes but to the interaction between oxalate and Lys side-chains being stronger than those existing in **α,γ-D6$_Z$**. Finally, dimer **α,γ-D6$_y$.(CO$_2$)$^{2-}$** could be switched back to the excimer-emitting form by the addition of morpholine (Dermer and Dermer 1937).

Conclusion

In summary, we have carried out a new self-assembly process based on an α,γ-CP that has precise control of the supramolecular ensemble and, at the same time, the three non-equivalent dimers can be inter-switched by addition of chemical signals that compete with the inter-strand salt bridge interaction present in the excimer-emitting dimer. The process is followed by the characteristic emission of a pyrene moiety linked to the CP. The design process could have applications in the development of sensors or molecular rotors through the introduction of appropriated substituents on amino acid side chains. Work is in progress to investigate this possibility further.

Acknowledgments This work was supported by the Spanish Ministry of Science and Innovation (MICINN) and the ERDF [SAF2007-61015, CTQ2007-68057-C02-01/BQU and Consolider Ingenio 2010 (CSD2007-00006)], the Xunta de Galicia (PGIDIT08CSA047209PR and GRC2010/012) and European project Magnifyco (NMP4-SL-2009-228622). MJPA thanks the Spanish MICINN for her PhD contract (FPI).

References

Amorín M, Castedo L, Granja JR (2003) New cyclic peptide assemblies with hydrophobic cavities: the structural and thermodynamic basis of a new class of peptide nanotubes. J Am Chem Soc 125:2844–2845

Amorín M, Castedo L, Granja JR (2005) Self-assembled peptide tubelets with 7Å pores. Chem Eur J 11:6543–6551

Amorín M, Castedo L, Granja JR (2008) Cyclic peptides folding control through N-methylation pattern selection: formation of antiparallel β-sheet dimers, double reverse turns and supramolecular helices by 3α,γ cyclic peptides. Chem Eur J 14:2100–2111

Ashkenasy N, Horne WS, Ghadiri MR (2006) Design of self-assembling peptide nanotubes with delocalized electronic states. Small 2:99–102

Bong DT, Clark TD, Granja JR, Ghadiri MR (2001) Self-assembling organic nanotubes. Angew Chem Int Ed 40:988–1011

Brea RJ, Amorín M, Castedo L, Granja JR (2005) Methyl-blocked dimeric α,γ-peptide nanotube segments: formation of a peptide heterodimer through backbone-backbone interactions. Angew Chem Int Ed 44:5710–5713

Brea RJ, López-Deber MP, Castedo L, Granja JR (2006) Synthesis of ω-(hetero)arylalkynylated α-amino acid by Sonogashira-type reactions in aqueous media. J Org Chem 71:7870–7873

Brea RJ, Castedo L, Granja JR (2007a) Large-diameter self-assembled dimers of α,γ-cyclic peptides, with the nanotubular solid-state structure of *cyclo*-[(*l*-Leu-*d*-^{Me}*N*-γ-Acp)$_4$-]·4CHCl$_2$COOH. Chem Commun (31):3267–3269

Brea RJ, Castedo L, Granja JR, Herranz MÁ, Sanchez L, Martín N, Seitz W, Guldi DM (2007b) Electron transfer in Me-blocked heterodimeric α,γ-peptide nanotubular donor-acceptor hybrids. Proc Natl Acad Sci USA 104:5291–5294

Brea RJ, Vázquez ME, Mosquera M, Castedo L, Granja JR (2007c) Controlling multiple fluorescent signal output in cyclic peptide-based supramolecular systems. J Am Chem Soc 129:1653–1657

Brea RJ, Reiriz C, Granja JR (2010) Towards functional bionanomaterials based on self-assembling cyclic peptides. Chem Soc Rev 39:1448–1456

Brea RJ, Pérez-Alvite MJ, Panciera M, Mosquera M, Castedo L, Granja JR (2011) Highly efficient and directional homo- and heterodimeric energy transfer materials based on fluorescently derivatized α,γ-cyclic octapeptides. Chem Asian J 6:110–121

Delphine CB, David MR, Jensen JH (2008) Very Fast Prediction and Rationalization of pKa Values for Protein-Ligand Complexes. Proteins 73:765–783

Dermer VH, Dermer OC (1937) Physical constants of morpholine. J Am Chem Soc 59:1148–1149

Garcia-Fandiño R, Granja JR, D'Abramo M, Orozco M (2009) Theoretical characterization of the dynamical behaviour and transport properties of α,γ-peptide nanotubes in solution. J Am Chem Soc 131:15678–15686

Hamley L (2007) Peptide fibrillization. Angew Chem Int Ed 46:8128–8147

Hui L, Andrew DR, Jensen JH (2005) Very Fast Empirical Prediction and Interpretation of Protein pKa Values. Proteins 61:704–721

Kashida H, Takatsu T, Sekiguchi K, Asanuma H (2010) An efficient FRET between pyrene and perylene assembled in a DNA duplex and its potential for discriminating single base changes. Chem Eur J 16:2479–2486

Khakshoor O, Nowick JS (2008) Artificial β-sheets: chemical models of β-sheets. Curr Opin Chem Biol 12:722–729

Knowles TP, Fitzpatrick AW, Meehan S, Mott HR, Vendruscolo M, Dobson CM, Welland ME (2007) Role of intermolecular forces in defining material properties of protein nanofibrils. Science 318:1900–1903

Kolstoe SE, Ridha BH, Bellotti V, Wang N, Robinson CV, Crutch SJ, Keir G, Kukkastenvehmas R, Gallimore JR, Hutchinson WL, Hawkins PN, Wood SP, Rossor MN, Pepys MB (2009) Molecular dissection of Alzheimer's disease neuropathology by depletion of serum amyloid P component. Proc Natl Acad Sci USA 106:7619–7623

König HM, Kilbinger AFM (2007) Learning from nature: β-sheet mimicking copolymers get organized. Angew Chem Int Ed 46:8334–8340

López-Deber MP, Castedo L, Granja JR (2001) Synthesis of N-(3-Arylpropyl)-amino acid derivatives by Sonogashira types of reaction in aqueous media. Org Lett 3:2823–2826

Martin RB (1996) Comparisons of indefinite self-association models. Chem Rev 96:3043–3064

Masuko M, Ohuchi S, Sode K, Ohtani H, Shimadzu A (2000) Fluorescence resonance energy transfer from pyrene to perylene labels for nucleic acid hybridisation assays under homogenous solution conditions. Nucleic Acids Res 28:e34

Matsui H, Gao X (2005) Peptide-Based Nanotubes in Bionanotechnology. Adv Mater 17:2037–2050

Nakamura M, Murakami Y, Sasa K, Hayashi H, Yamada K (2008) Pyrene-zipper array assembled via RNA duplex formation. J Am Chem Soc 130:6904–6905

Neuman KC, Nagy A (2008) Single-molecule force spectroscopy: Optical tweezers, magnetic tweezers and atomic force microscopy. Nature Methods 5:491–505

Park JW, Song HE, Lee SY (2003) Homodimerization and heteroassociation of 6-*O*-(2-sulfonato-6-naphthyl)-γ-cyclodextrin and 6-deoxy-(pyrene-1-carboxamido)-β-cyclodextrin. J Org Chem 68:7071–7076

Pazos E, Vázquez O, Mascareñas JL, Vázquez ME (2009) Peptide-based fluorescent biosensors. Chem Soc Rev 38:3348–3359

Reiriz C, Brea RJ, Arranz R, Carrascosa JL, Garibotti A, Manning B, Valpuesta JM, Eritja R, Castedo L, Granja JR (2009) α,γ-Peptide nanotube templating of 1D parallel fullerene arrangements. J Am Chem Soc 131:11335–11337

Remaut H, Waksman G (2006) Protein–protein interaction through beta-strand addition. Trends Biochem Sci 31:436–444

Roy R, Hohng S, Ha T (2008) A practical guide to single-molecule FRET. Nature Methods 5:507–516

Searle MS, Ciani B (2004) Design of β-sheet systems for understanding the thermodynamics and kinetics of protein folding. Curr Opin Struct Biol 14:458–464

Shiraishi Y, Tokitoh Y, Hirai T (2006) pH- and H_2O-driven triple-mode pyrene fluorescence. Org Lett 8:3841–3844

Smeenk JM, Otten MBJ, Thies J, Tirrell DA, Stunnenberg HG, van Hest JCM (2005) Controlled assembly of macromolecular β-sheet fibrils. Angew Chem Int Ed 44:1968–1971

Stefani M, Dobson CM (2003) Protein aggregation and aggregate toxicity: new insights into protein folding, misfolding diseases and biological evolution. J Mol Med 81:678–699

Ulijn RV, Smith AM (2008) Designing Peptide Based Nanomaterials. Chem Soc Rev 37:664–675

Valeur B (2002) Molecular fluorescence. Wiley, Weinheim

Whitehouse C, Fang J, Aggeli A, Bell M, Brydson R, Fishwick CWG, Henderson JR, Knobler CM, Owens RW, Thomson NH, Smith DA, Boden N (2005) Adsorption and self-assembly of peptides on mica substrates. Angew Chem Int Ed 44:1965–1968

Zhang S (2003) Fabrication of novel materials through molecular self-assembly. Nat Biotechnol 21:1171–1178

Zhang X, Rehm S, Safont-Sempere MM, Würthner F (2009) Nature Chem 1:623–629